Post Buckling Behavior of Steel Plate Girder Panels Under Shear Loading

Hassan Ghanem, Safwan Chahal[(✉)], Wafik Ajam, and Adel Kurdi

Beirut Arab University, Beirut, Lebanon
h.ghanem@bau.edu.lb, safwanchahal79@gmail.com

Abstract. Previously, the shear design of web and transverse stiffeners was based on the initial shear buckling in the web without the tension field action. The American Institute of Steel Construction (AISC) adopted post-buckling tension field strength into its specifications for stiffened interior web panels but exclude the post-buckling tension field action for the end web panel. In this study, a finite element method (FEM) analysis on an isolated panel confirms the view that post-buckling strength of steel plate girders is attributed to a non-uniform shear stress distribution along the boundary of the plates, varying from the critical stress in one corner up to the shear-yield stress in the tension corner with no need for any diagonal tension. It was also shown that the presence of flanges with bending strength does rise the shear capacity in the panel. However; light flanges give a slight increase in shear resistance without diagonal tension, but heavy flanges are shown to be capable of developing true diagonal tension, leading to a significant gain in total shear capacity.

Keywords: Shear stress · Buckling · Tension field action

1 Introduction

When a web is subjected to shear, before it buckles, equal tensile and compressive principal stresses are developed within the plate. If the applied loading is increased, the buckling of the plate does not limit the shear resistance [1–4].

The post buckling strength was first attributed by Wagner in 1929 to a complete uniform tension field reacted by rigid flanges [5]. Basler in 1961 observed that in welded plate girders, the flanges are too flexible to resist the web tension, and he proposed a partial tension field anchored against the vertical edges of the panel [6]. The Wagner and Basler models represent the two extreme cases of the many models that have been proposed that make use of the idea of diagonal tension. Marsh suggested a different model in which, after initial buckling, the uniform shear distribution along the boundary changes, with increasing shear stress toward the tension corner, but with no stress normal to any boundary [7].

Marsh and Ajam use the finite element approach and obtained a numerical solution that can be formulated in terms of simple physical concepts [8]. A classical stability analysis for the critical shear stress in a web is based on a uniform shear-stress distribution. In practice, for a thin web, a uniform distribution of the stress is not possible if there are initial imperfections [9–11]. As the buckled plates deflect further, the non-

uniformity stresses at the edges increase and the resistance to shear force is provided by pure shear stress along the boundaries, which, in the limit, varies from approximately the initial buckling stress at the compressive corners, to the yield stress in shear in the tension corners, where the short compressive strips are sufficiently stable [12–14].

An isolated panel subjected to shear distortion is capable of carrying a shear force well in excess of that causing initial shear buckling, even when the boundary flanges have no bending strength.

This study covers two conditions of end panels: 1-Shear capacity for a square panel with flanges that have area (axial stiffness) but no flexural stiffness. 2-Behavior and shear capacity of a square panel with flexural stiffness flanges.

2   Square Panels with Flanges That Have No Bending or Torsional Stiffness

The initial analysis is for a single square panel with stiffeners along all four edges, the stiffeners having an area, and hence axial stiffness, but no flexural rigidity (β). When this panel is subjected to a shear force, it is evident that there can be no normal stress at the boundaries and only shear stress can exist there.

ABAQUS program was used in the analysis. Rather than applying a shear loading, imposed displacements of the stiffeners are used. In Fig. 1, the distance OA′ is reduced, and distance OB is increased, by an amount δ, causing a shear displacement along the boundary, leading to a shear stress distribution which will be determined by the analysis.
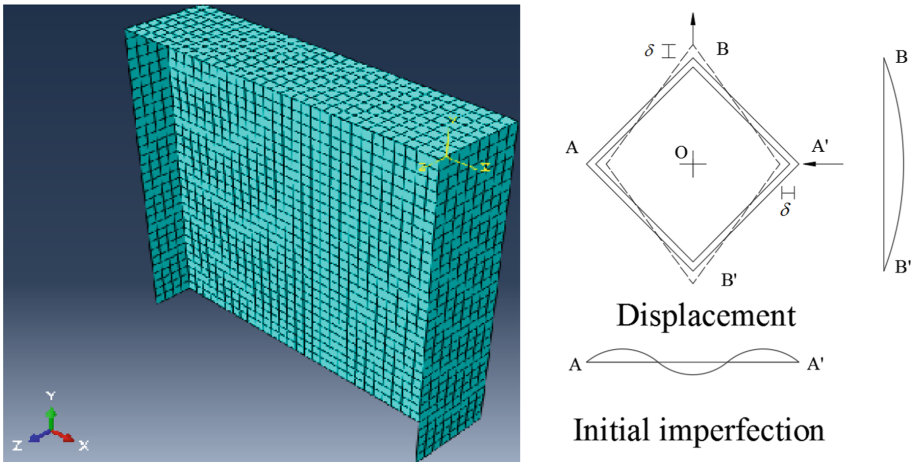
Fig. 1. A square plate finite element grid, 30 × 30 elements with light flanges.

For a square panel, of depth d and thickness t, subjected to a uniform shear distribution the elastic buckling stress, τ_{cr} is given by:

$$\tau_{cr} = 9.34\,\pi\,E\,t^2/(12(1-v)d^2) \tag{1}$$

Where v is the Poisson's ratio and E is the modulus of elasticity. The total shear force at initial elastic buckling is equal to:

$$V_{cr} = \tau_{cr}dt \tag{2}$$

After buckling, as the applied displacement increases, the shear stress is no longer uniform but increases in value towards the tension corner. This process is continued until the web yields in shear at the corner. The total shear force V, is given by the integration of the shear flux along the boundary. For more displacement of the flanges the extent of the yield zone increases, but for the case with flanges having no flexural stiffness, the actual total shear force along the boundary has been shown to decrease, due to a change in the stress distribution.

Figure 2 shows the variation of the central deflection w/t with respect to the shear displacements. Irrespective of the assumed initial central deflection, the central deflection increases only when the imposed shear displacement reaches a certain critical value τ_{cr}. This point is the bifurcation point and it agrees very well the linear buckling theory.
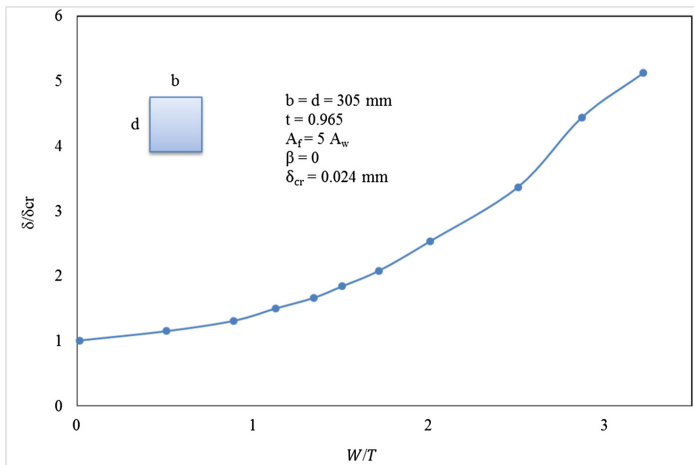
Fig. 2. Relation between shear displacement and center deflection

At the bifurcation point the plate deflection is formed by three half-waves in the compression direction and one half-wave in the tension direction. For non-dimensional presentation of the results, the value on the abscissa is the ratio $\Delta = \delta / \delta_y$, where δ_y is the nominal displacement when the shearing strain is τ_y/G given by:

$$\delta_y = (d/2\sqrt{2})(\tau_y/G) \tag{3}$$

Where G is the elastic shear modulus. The ordinate is V/V_y, where V is the total shear force and $V_y = \tau_y dt$.

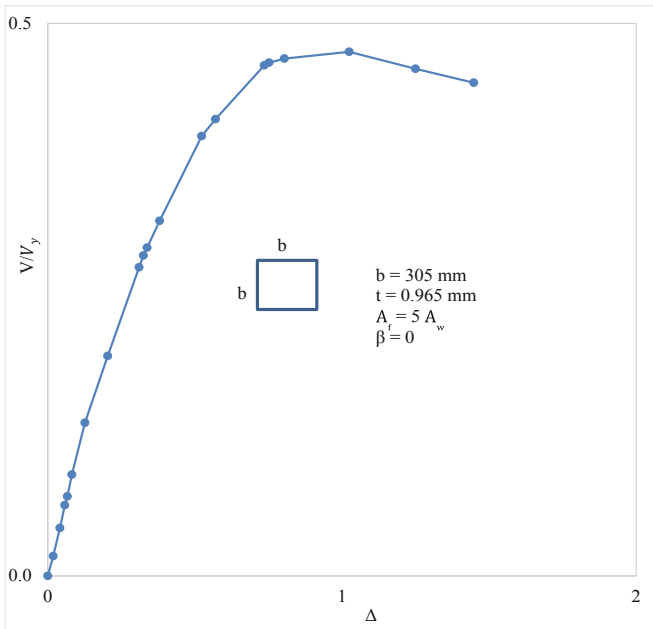Figure 3 shows the behavior of a panel with $d/t = 316$. t = 1 mm, and a flange area $A_f = 5A_w = 5dt$.

Fig. 3. Shear force V displacement

The variation of the shear stress along the boundary is shown in Fig. 4. The abscissa is the ratio x/b, and the ordinate is τ/τ_y.

Figure 5 shows the ratio of the central deflection to the thickness plotted along the compression diagonal, for various displacement values. As shown, the deflection is formed by three half waves in the compression direction.

The proposed model in square panel resembles two sets of diagonal strips, one in tension and in compression; limiting to τ_{cr} at the longest compression diagonal and τ_y at the longest tension diagonal. It is assumed that the buckling stress at the boundaries varies in parabolic form as shown in Fig. 6, the shear stress at a point on the edge is:

$$\tau_s = \tau_{cr} + (\tau_y - \tau_{cr})\,(x/d)^2 \tag{4}$$

In which x = distance from the corner; τ_{cr} = theoretical critical shear stress which occurs at x = Zero, and τ_y = yielding shear stress which occurs at x = d.
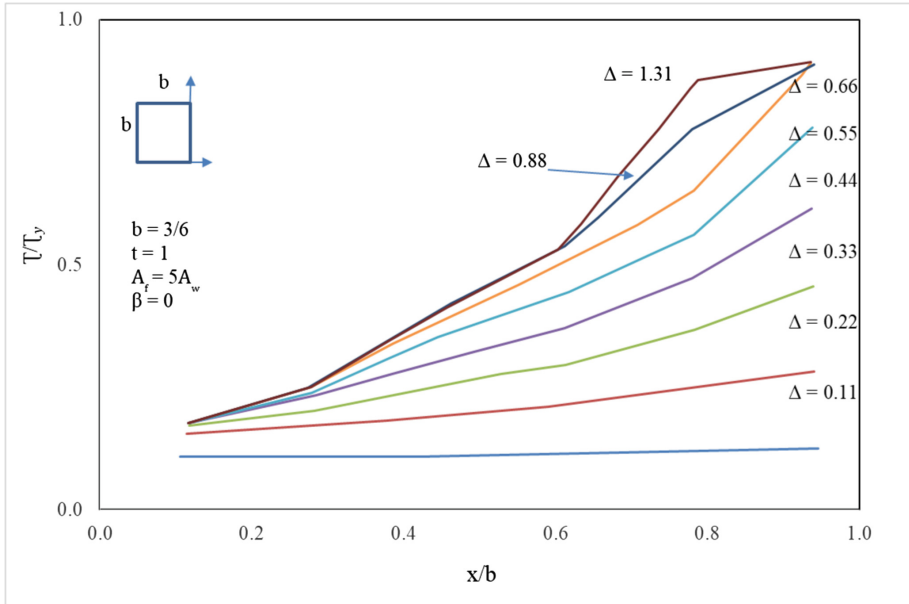
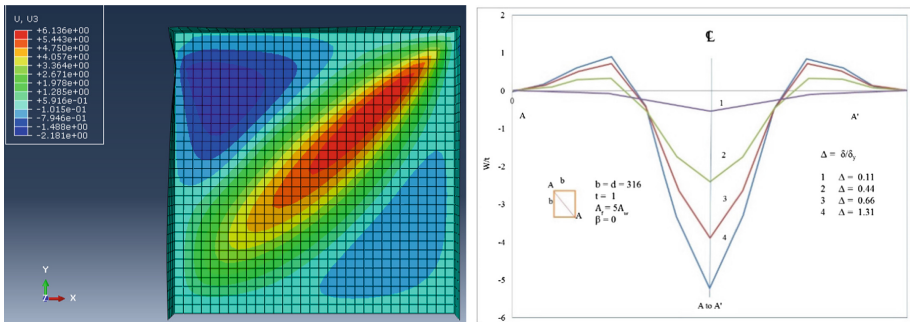**Fig. 4.** Shear stress along boundary for varying displacement

Fig. 5. Deflection along compression diagonal

The principal stress along any line running at 45° remains constant along that line, with a maximum value of $\sigma_c = \sigma_t = \tau_y$. At any point in the web, for values of $(x+y)<d, x<y$, the stresses are given by:

$$\sigma_c = \tau_{cr} + (\tau_y - \tau_{cr})\left((x-y)/d\right)^2 \tag{5}$$

$$\sigma_t = \tau_{cr} + (\tau_y - \tau_{cr})\left((x+y)/d\right)^2 \tag{6}$$
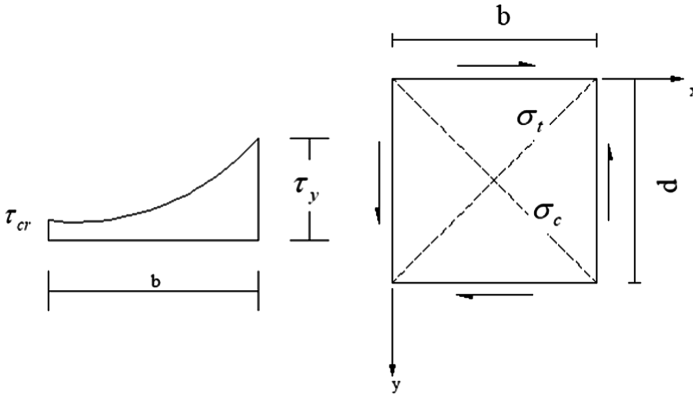
Fig. 6. Square panel under shear force in the proposed model

$$\tau_{xy} = \tau_{cr} + (1/2)\,(\tau_y - \tau_{cr})\,((x-y)^2 + (x+y)^2)/d^2 \tag{7}$$

The shear force V on a boundary is the area under the shear stress - thickness curve.

$$V = t \int_0^d \tau_s dx \tag{8}$$

The critical shear stress depends upon the boundary conditions of the isolated panel, but the true boundary conditions for a girder web are difficult to establish accurately because the degree of restraint imposed by the flanges and by the adjacent web panels cannot be evaluated. It can be assumed conservatively that all the boundaries of the web panel are simply supported.

Up to first yield, Eq. 4 represents the variation of the shear stress along the boundaries. The shear forces in the plate at first yield in the web is obtained by integrating the shear stress distribution along the edge, giving:

$$V_w = (1/3)(2\tau_{cr} + \tau_y)dt \tag{9}$$

For more rigid flanges the ultimate shear force is equal to the shear force up to first yielding plus the contribution of the flanges in shear.

The failure load can be determined from a consideration of the mechanism developed in the frame panel. In this model, up to first yielding in shear there is no normal force at the boundary. As the load increases, σ_t will increase and σ_c will reduce in such way as to conserve the value of shear stress τ_y at the tension corner, as the normal force increases. The tension stress in the longer diagonal increases up to the value of σ_y, the final condition approaching a series of yielded diagonals strips that maximum value of the normal force developed at the boundary is t $\sigma_y/2$.

3   Square Panels with Flanges That Have Rigidity

A finite element analysis was conducted, for a panel with a high slenderness ratio with flexural rigidity as shown in Fig. 7. The two tension corners are free to move; one compression corner is fixed in the X and Y directions. The load is applied at the other compression corner in X and Y direction. The relative proportions of the flange are expressed by the ratio of flange area to web area A_f/A_w and the ratio β, of plastic moment strength of the flange $(0.25b_f\ t_f^2\ \tau_y)$ to that required to resist a tension field encompassing the whole panel, with an interior hinge at the midpoint $(c_yb^2t/32)$, this $β = 8b_f\ t_f^2\ /b^2t$, which is usually less than 0.1 for practical welded plate girders.
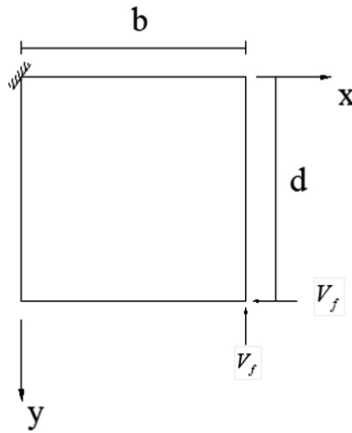

Fig. 7. Finite element test for square panel under compression load at one corner

After first yielding in shear at the tension corner, as the load increases the yielded zone spreads, and normal forces are created on the flanges. Failure occurs when the hinges have formed in the flanges which together with the yielded zone A A′ A″, B B′ B″ form a plastic mechanism as shown in Fig. 8.

By considering a rotation ø to occur at the plastic hinges producing the mechanism shown in Fig. 9, the work done in the plastic deformation of the flange and web is:

$$2V_fc\phi = 8M_p\phi + 4(\sigma_y/2)ctc\phi/2$$
$$V_f = 4M_p/c + ct\sigma_y/2 \tag{10}$$

The load is applied at the compression corner in Fig. 9 in the Y direction only, and is assumed to be reacted by a uniformly distributed load $\sigma_y\ t/2$ normal to the flange exerted by the web. Since the plastic hinge will occur at the point of maximum bending
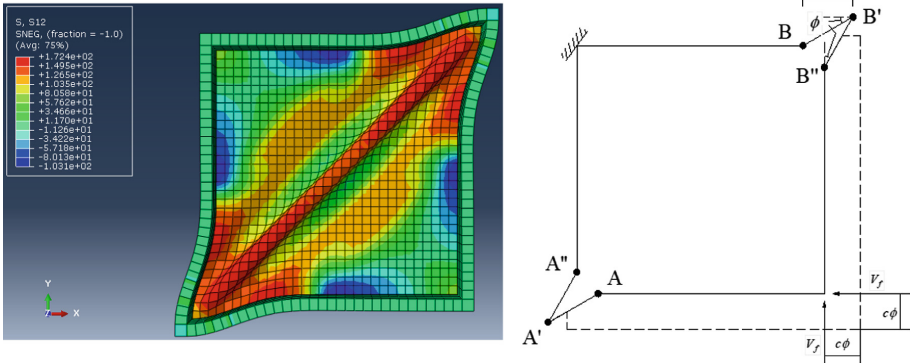
Fig. 8. Hinge formation in the flange of isolated panel
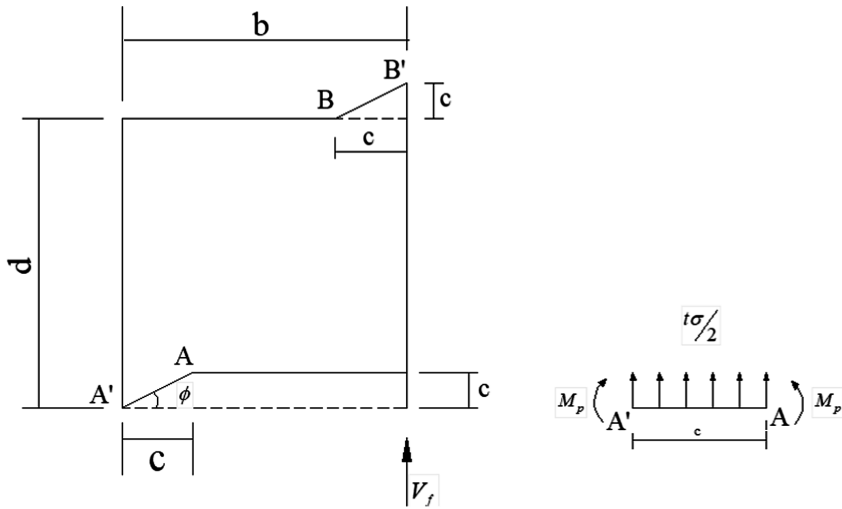
Fig. 9. Formation of two hinges in the flange

moment where the shear is zero, the position of the internal hinge A is obtained by considering the equilibrium of the beam section A A'. Taking moments about A', one obtains:

$$(ct\sigma_y/2)c/2 = 2\,M_p \Rightarrow 4M_p/c = ct\sigma_y/2$$
$$c = \sqrt{(8\,M_p(\sigma_y t)}$$

(11)

The failure load will be equal to the force at first yield plus the contribution of the flange when the normal forces are developed.

$$V_u = V_w + V_f \tag{12}$$

In the case of a girder, the internal hinges A″ and B″ will not be formed because we have a continuous web, and the failure load will be determined from a consideration of the mechanism developed in Fig. 9. Consider a rotation ø at the plastic hinges, the work is done only on the sections AA′ and B B′. For equal flanges, the distance c for upper and lower flanges will be equal, and the work done by the axial force in the flanges will be zero.

The virtual work done in the mechanism is:

$$
\begin{aligned}
V_f c\phi &= 4M_p\phi + [2(\sigma_y/2)(ct)/2](c\phi) \\
V_f &= 4M_p/c + (\sigma_y/2)(ct)
\end{aligned}
\tag{13}
$$

Equation 13 is the same as Eq. 10. The first term of this equation, on the right-hand side, represents the frame resistance in shear, the second term represents the contribution of the flanges to increasing the web capacity. By using Eq. 11 these two terms are shown to be equal. Putting Eqs. 9 and 10 into Eq. 12 gives.

$$V_u = (1/3)(2\tau_{cr} + \tau_y)dt + \sigma_y ct \tag{14}$$

Using the value of c from Eq. 11 in Eq. 14 the ultimate shear force becomes:

$$V_u = (1/3)(2\tau_{cr} + \tau_y)dt + \sqrt{8M_p\sigma_y t} \tag{15}$$

It should be noted that the value of the plastic moment in the flange will be reduced by the presence of the axial force P′. The value of the effective moment M′ is given by:

$$M' = M_p(1 - (P'/P)^2) \tag{16}$$

Where P is the axial force to yield the flange, equal to $A_f\sigma_y$.

4 Extreme Cases

From Eq. 14, it can be seen that the shear capacity is composed of two components. The first component represents the capacity of the web up to first yield without any contribution from the flange; the second component represents the additional shear capacity of the flange bending rigidity.

In the case of a girder with very weak flanges, taking account of the reduced moment resistance due to the axial force in the flange, the value of the flange strength M_p becomes small and the value of c becomes very small; the second term of Eq. 13 becomes negligible so that.

$$V_u = (1/3)(2\tau_{cr} + \tau_y)dt \tag{17}$$

When the flanges are very strong, the distance of the plastic hinge from the end of the panel c increases, as shown by Eq. 11. When c because equal to the width b, the hinges form at the four corners of the panel to form a "picture frame" mechanism, as shown in Fig. 10.
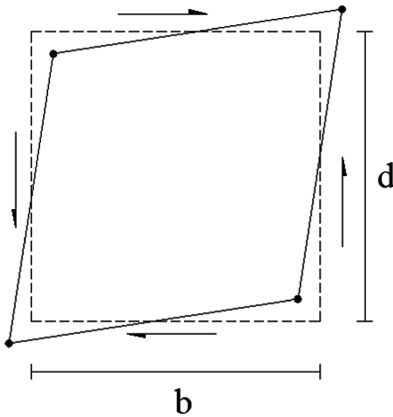
Fig. 10. Hinge formation at all corners of the panel

By substituting the value of c = b = d into Eq. 11 we get:

$$M_p = d^2 \sigma_y t / 8 \tag{18}$$

When determining the ultimate shear load for any girder, the flange strength should be evaluated to see whether it exceeds the limiting value given by Eq. 18. If this is so (it will not often be the case for girders of civil engineering proportions), the expression for shear capacity is:

$$V_u = ((1/3)(2\tau_{cr} + \tau_y) + \sigma_y)dt \tag{19}$$

5   Comparison of Predicted Shear Strength

Table 1 gives the properties of the plate girder panels. Table 2 gives comparisons of predicted shear strengths according to the present model with results of tests from a number of sources. Table 3 summarized the comparison of test results.

Table 1. Properties of square panels

Ref	Girder	t mm	d mm	A_w	t_f mm	b_f mm	A_f/A_w	β
15	TG1	2.72	609.8	1658.0	4.70	101.6	0.29	0.018
15	TG2	2.72	609.8	1658.0	6.55	101.6	0.40	0.034
15	TG14	.965	304.8	294.0	3.12	76.2	0.81	0.093
15	TG15	.965	304.8	294.0	5.00	76.2	1.30	0.224
15	TG16	.965	304.8	294.0	6.45	76.2	1.67	0.451
15	TG17	**.9**65	304.8	294.0	9.32	76.2	2.41	0.850
15	TG18	.965	304.8	294.0	12.95	76.2	3.36	1.593
15	TG19	.965	304.8	294.0	15.52	76.2	4.02	2.004
15	TG20	2.03	304.8	619.0.	3.25	76.2	0.40	0.046
15	TG21	2.03	304.8	619.0.	4.88	76.2	0.60	0.097
15	TG22	2.03	304.8	619.0.	6.48	76.2	0.80	0.207
15	TG23	2.03	304.8	619.0.	9.22	76.2	1.14	0.419
15	TG24	2.03	304.8	619.0.	12.95	76.2	1.59	0.724
15	TG25	2.03	304.8	619.0.	15.54	76.2	1.91	0.914
15	G7T1	4.98	1270.0	6325.0	19.50	310.0	0.96	0.120
16	TG1′	2.50	1000.0	2500.0	5.06	160.0	0.32	0.019
16	TG2′	2.50	1000.0	2500.0	10.00	200.0	0.80	0.090
16	TG3′	2.50	1000.0	2500.0	16.43	200.0	1.31	0.241
16	TG4′	2.50	1000.0	2500.0	20.16	200.0	1.61	0.366
16	TG5′	2.50	1000.0	2500.0	29.73	200.0	3.00	0.790
17	PC3	1.0	800.0	800.0	10.0	250.0	3.12	0.431

Table 2. Comparison between test results, P.D.P, Hoglund [18] and Rockey [15]

Girder	d/t	σ_y MPa	σ_{yf} MPa	V P.D. P. KN	V Hoglund KN	V Rockey KN	V Exp KN
TG1	224	253	253	120.0	140.0	143.0	120.0
TG2	224	253	253	130.0	138.0	142.0	126.0
TG14	361	219	309	24.0	21.0	23.0	25.0
TG15	.361	219	289	29.0	24.0	26.0	29.0
TG16	361	219	249	35.0	29.0	30.0	31.0
TG17	.361	219	315	43.0	37.0	36.0	39.0
TG18	361	219	306	54.0	46.0	44.0	51.0
TG19	.361	219	268	59.0	50.0	48.0	55.0
TG20	150	229	.309	65.0	64.0	68.0	51.0
TG21	150	229	289	73.0	67.0	71.0	71.0
TG22	150	229	.349	84.0	74.0	76.0	79.0
TG23	150	229	.315	96.0	83.0	81.0	81.0
TG24	150	229	.306	114.0	99.0	90.0	96.0
TG25	150	229	.268	121.0	106.0	94.0	104.0

Table 2. (*continued*)

Girder	d/t	σ_y MPa	σ_{yf} MPa	V P.D. P. KN	V Hoglund KN	V Rockey KN	V Exp KN
G7T1	255	253	259	645.0	575.0	605.0	623.0
TG1′	400	200	280	131.0	119.0	142.0	152.0
TG2′	400	200	280	174.0	136.0	166.0	160.0
TG3′	400	200	280	223.0	168.0	196.0	190.0
TG4′	400	200	280	251.0	191.0	214.0	219.0
TG5′	400	200	280	323.0	256.0	265.0	309.0
PC3	800	216	362	82.0	49.0	73.0	79.0

Table 3. Ratio of predicted to experimental capacity

Investigator	Mean of V_u/V_{ex}	Standard deviation	Range of V_u/V_{ex}
Hoglund	0.91	0.17	0.62–1.17
Rockey	0.97	0.11	0.82–1.22
P.D.P	1.08	0.11	0.86–1.25

6   Conclusion

The finite element method has been used for the large deflection elastic-plastic analysis of plates under shear loading, in the post-buckled regime. This study is focused on the distribution of the stress along the boundaries after buckling in shear, the prediction of the ultimate shear force and the influence of flange strength on the ultimate shear resistance. The following points can be made:

- Prior to buckling, the shear stress is uniformly distributed along the boundary. After buckling, the shear stress distribution becomes non-uniform with a maximum value at the tension corner. Up to the shear force which causes first yielding at the junction between the web and the flange at the tension corner, there is no normal force at the boundaries.
- In most girders used in civil engineering the flanges are light and no useful diagonal tension is developed before the maximum capacity is reached.
- When the d/t ratio of the panel is small enough that the shear force to cause yielding exceeds that to cause elastic bucking, no bending is developed in the flanges. The first yield may take place in the middle of the panel area, due to a combination of membrane stress and bending stresses.
- The proposed model to predict the ultimate load capacity shear webs in a plate girder treats the shear strength of the web and the bending strength of the flanges independently.
- The proposed equation is simple, applies to square panels, give satisfactory results compared with many tests, and avoids the need for iteration used in other methods.

References

1. Glassman, J., Moreyra Garlock, M.: A compression model for ultimate postbuckling shear strength. Thin-Walled Struct. **102**, 258–272 (2016)
2. Alinia, M., Gheitasi, A., Shakiba, M.: Postbuckling and ultimate state of stresses in steel plate girders. Thin-Walled Struct. **49**(4), 455–464 (2011)
3. Alinia, M., Shakiba, M., Habashi, H.: Shear failure characteristics of steel plate girders. Thin-Walled Struct. **47**(12), 1498–1506 (2009)
4. Takeda, H., Watanabe, E., Kunishi, R.: Inelastic repetitive shear and flexural buckling of plate girders. Int. J. Struct. Stab. Dyn. **04**(01), 105–124 (2004)
5. Marsh, C.: Theoretical model for collapse of shear webs. J. Mech. Eng. ASCE **108**(5), 819–832 (1982)
6. Basler, K.: Strength of plate girders in shear. ASCE, Proc. No 2967, Part 1, ST 7, pp. 151–180 (1969)
7. Marsh, C.: Photoelastic study of postbuckled shear webs. Can. J. Civ. Eng. **12**(2), 415–417 (1985)
8. Marsh, C., Ajam, W.: Post-buckling strength of shear webs without diagonal tension. In: International Conference on Steel & Aluminium Structure, Cardiff, U.K (1987)
9. Berman, J., Bruneau, M.: Plastic analysis and design of steel plate shear walls. J. Struct. Eng. **129**(11), 1448–1456 (2003)
10. de Béjar, L., Younis, M.: Shear strength of open-web plate girders with inclined tension bars. J. Eng. Mech. **117**(11), 2699–2719 (1991)
11. White, D., Barker, M.: Shear resistance of transversely stiffened steel I-Girders. J. Struct. Eng. **134**(9), 1425–1436 (2008)
12. Yoo, C., Lee, S.: Mechanics of web panel postbuckling behavior in shear. J. Struct. Eng. **132**(10), 1580–1589 (2006)
13. Lee, S., Yoo, C., Yoon, D.: Behavior of intermediate transverse stiffeners attached on web panels. J. Struct. Eng. **128**(3), 337–345 (2002)
14. Lee, S., Yoo, C.: Experimental study on ultimate shear strength of web panels. J. Struct. Eng. **125**(8), 838–846 (1999)
15. Rockey, K.C., Skaloud, M.: The ultimate load behavior of plate girders loaded in shear. J. Struct. Engr. **50**(1), 29–47 (1972)
16. Sadao, K.: Ultimate strength of stiffened plate subjected to shear. In: Proceedings of the IABSE Colloquium, London (1971)
17. Tang, K.H., Evans, H.R.: Transverse Stiffeners for plate girders wens an experimental study. J. Const. Steel Res. 4, 253–280
18. Hoglund, T.: Simply supported long thin plate girders without web stiffeners subjected to distributed transverse load. In: Proceedings of the IABSE Colloquium, London (1971)